ORBIT-SPIN COUPLING AND THE CIRCULATIONS OF PLANETARY ATMOSPHERES: INSIGHTS GAINED FROM NUMERICAL MODELING WITH THE MarsWRF GCM

J. H. Shirley, *Jet Propulsion Laboratory, California Institute of Technology, Pasadena CA USA (jshirley@jpl.nasa.gov),* **M. A. Mischna,** *Jet Propulsion Laboratory, California Institute of Technology, Pasadena CA USA.*

Introduction:

A new physical hypothesis bearing on the observed inter-annual variability of the Mars atmosphere has been developed and tested through numerical modeling with the MarsWRF General Circulation Model (GCM) [*Shirley*, 2016; *Mischna and Shirley*, 2016]. Some aspects of the physical hypothesis are novel and may therefore be unfamiliar to the atmospheric community. The primary goal of this presentation is to review and discuss the essential features of the new hypothesis. This abstract outlines a sequence of topics that may be addressed during our presentation, depending on the time available. We first briefly summarize the physical hypothesis without dwelling on its origins or derivation. We then describe a few key features of the predicted acceleration field and its variability with time. We conclude with a comparison between outcomes of MarsWRF modeling runs performed both with and without the predicted accelerations.

Physical hypothesis: Orbital and rotational motions of extended bodies (Fig. 1) are traditionally considered to occur independently (without any form of coupling or interference). A weak coupling of these motions is proposed in *Shirley* [2015, 2016].

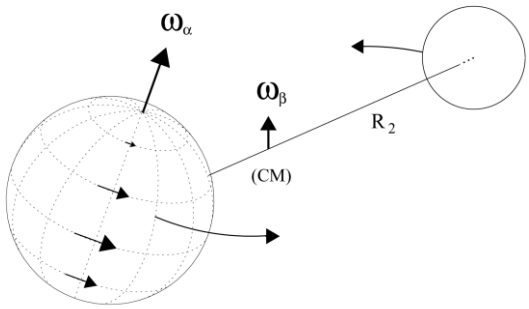

Figure 1. Rotation and revolution in a 2-body system. The curved arrows represent the orbital trajectories of a subject body (at left) and its companion as they revolve about the center of mass (CM) or *barycenter* of the pair. The orbital motion is also represented by the angular velocity vector ω_β, which is normal to the orbital plane. **R** denotes the orbital radius extending from the body center to the barycenter, here labeled only for the companion body. The axial rotation of the subject body is parameterized by the angular velocity vector ω_α.

The Mars atmosphere is suspected to play an important role in the coupling process. The "coupling term acceleration" (*CTA*) is given by the following equation:

$$CTA = -c(\dot{L} \times \omega_\alpha) \times r$$

Here $\boldsymbol{\omega_\alpha}$ is the angular velocity of the planetary axial rotation and $\dot{\boldsymbol{L}}$ is the time derivative of the orbital angular momentum with respect to the solar system barycenter. Crossing this vector product with a position vector, *r*, yields the local coupling term acceleration (*CTA*) vector at each location (grid point) on or above the surface. *c* quantifies the efficiency of the exchange of momentum between orbital and rotational reservoirs. Solar system observations constrain the value of *c* to be extremely small (otherwise planetary motions and rotations would vary more substantially, in ways that are not observed).

Figure 2 illustrates the acceleration field predicted by the above equation, for one moment in time.

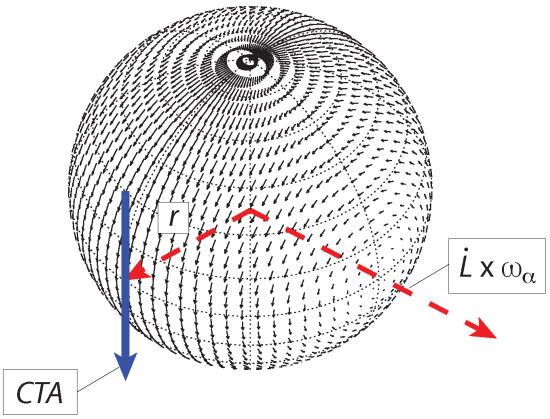

Figure 2. Vector representation of the CTA accelerations over the surface of an extended body, for the MarsWRF grid points employed. The lengths of the displayed vectors are proportional to their magnitude. Latitude and longitude grid lines at 15° intervals are shown for reference.

Spatial and temporal variability of the acceleration field on diurnal time scales:

First let us visualize the axial rotation of the body carrying a particular surface location through the illustrated pattern (or *field*) of accelerations once per day. Consider the vectors plotted for points on the northernmost latitude circle (i.e., 60^{o} N). As the body rotates, the acceleration points northward, then eastward, then southward, then westward, varying systematically in magnitude through this interval.

This diurnal pattern of variability combines in a somewhat complex fashion with the normal diurnal cycle of solar heating that is responsible for driving both dayside convective activity and the well-known thermal tidal cycles of the Mars atmosphere. To see how this occurs, let us next suppose that a portion of the globe of Fig. 2 is illuminated by radiation from the Sun. Over the period of one year, the "sunlit hemisphere" of Mars would progress through a complete rotation, with respect to the approximately fixed pattern of accelerations shown in Fig. 2. If the resolved accelerations are directed northward at local noon in a particular location, then (holding all else constant, for purposes of illustration), approximately 6 (Mars) months later they would be directed southward at that same local time.

Temporal variability of the forcing function:

In addition to the diurnal variability noted above, we also recognize that both the sign and the magnitude of the *CTA* scale directly with the rate of change of the planetary orbital angular momentum, $\dot{\boldsymbol{L}}$. The variability of this parameter in the case of Mars over the period from 1980 to 2000 is illustrated in Fig. 3.

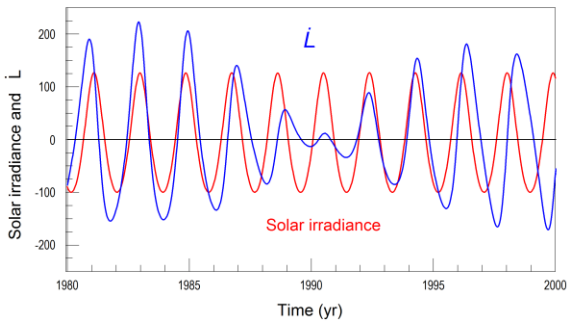

Figure 3. Phasing of the waveforms of the rate of change of the orbital angular momentum of Mars ($\dot{\boldsymbol{L}}$, in blue) and the solar irradiance at Mars (in red) from 1980-2000. Units on the y-axis correspond to deviations from the mean value of the solar irradiance at Mars (~590 W m^{-2}). The $\dot{\boldsymbol{L}}$ waveform has been arbitrarily scaled for purposes of illustration. It attains positive and negative extrema of 4.45 x10^{6} M_{Mars} m^{2} s^{-2} and -3.41 x10^{6} M_{Mars} m^{2} s^{-2} during this interval.

The variability of the amplitude and period of the $\dot{\boldsymbol{L}}$ waveform is due to solar system dynamics, as described in *Shirley* [2015]. As a consequence of this variability, the CTA acceleration field periodically disappears (as the forcing function $\dot{\boldsymbol{L}}$ passes through the zero points of the curve of Fig. 3), to subsequently re-emerge with opposite sign. The directions of all of the local acceleration vectors of Fig. 2 would then be *reversed*, as a consequence of this form of variability.

From the above considerations, we are led to the most basic prediction of the orbit-spin coupling hypothesis: That the subject atmosphere will experience cycles of intensified large scale motions, centered near the extrema of the $\dot{\boldsymbol{L}}$ waveform; while conversely "relaxing" to an unforced state, during intervals when the $\dot{\boldsymbol{L}}$ waveform approaches and transitions through the zero points.

Figure 3 also illustrates the annual cycle of solar irradiance over the same time interval. The incommensurability of the periods of the $\dot{\boldsymbol{L}}$ waveform and the solar year leads to continuous variability of the phasing of the two curves illustrated. According to the hypothesis under evaluation, the variable phasing of the $\dot{\boldsymbol{L}}$ waveform with respect to the annual cycle may play an important role in contributing to the inter-annual variability of the atmospheric circulation of Mars.

Comparisons of forced and unforced MarsWRF GCM outcomes:

The coupling term accelerations have been incorporated within the dynamical core of the MarsWRF GCM. The resulting modified GCM has been subjected to extensive validation and testing [*Mischna and Shirley*, 2016]. Introduction of this added forcing within the already complex dynamics of a general circulation model may lead to consequences and phenomena that are difficult to foresee. However, in the above-cited study, we found that conditions favorable to the occurrence of global-scale dust storms (GDS) were generally reproduced by the model, for years in which known past perihelion-season GDS actually occurred.

An important caveat for the present version of the GCM is that all of the model runs thus far reported have been performed with atmospheric dust "turned off," in order to best isolate the consequences of the *CTA*. (However, please also see the presentations by *Mischna et al.* and *Newman et al.*, this conference). Work is now underway to describe the effects of both passive and active dust within the models as forced by the CTA. Secondly, to date we have left the model parameterizations of the Mars water cycle in their default states. We recognize that a great deal remains to be done before we can claim a realistic simulation of atmospheric conditions on Mars with the modified MarsWRF model.

Comparison of global wind fields in forced and unforced model runs:

The following two figures illustrate differences in

wind fields observed between the forced and unforced versions of the GCM, for a specific date within the southern spring season of the Mars year.

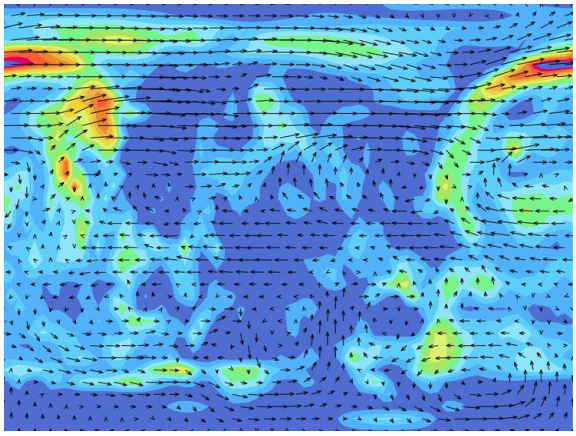

Figure 4. Unforced (baseline) MarsWRF simulation for Ls=217°. Color: surface wind stress (Pa). Arrows: Wind speed at ~1 scale height, illustrating wind directions in the lower atmosphere. Areas of high wind stress are seen in the northern highlands, to the northwest of Alba Patera and over the northern portions of Tharsis, and to the southeast of the Hellas basin. The equatorial winds are dominated by easterly flow, while those of northern high latitudes show the strong westerly flow appropriate for this season.

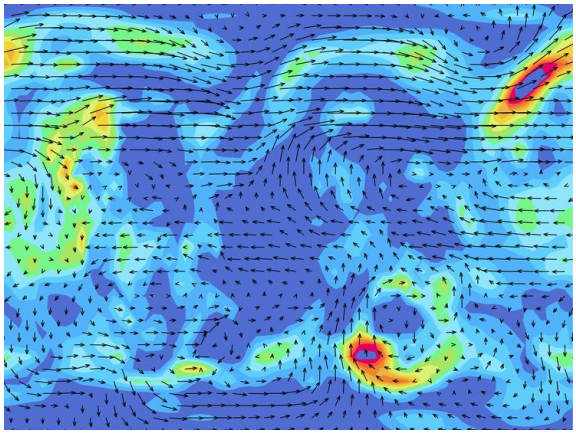

Figure 5. MarsWRF simulation for Ls=217° of MY 28, with coupling term accelerations (CTA) included [Mischna and Shirley, 2016]. Color shading indicates surface wind stress and arrows identify wind directions at ~1 scale height (as in the prior figure). The locations of the highest resolved surface wind stresses differ from those of the prior figure, and the wind field is strikingly different, with substantially greater meridional components of motion in evidence in many locations.

The wind field of Fig. 5 corresponds to a period of "intensification" of the large-scale circulation, under the hypothesis under evaluation, as the $\dot{\boldsymbol{L}}$ waveform for this date was nearing a positive extreme value. The winds at one scale height exhibit stronger meridional components than is the case for the unforced simulation of Fig. 4. Northward winds to the west of the Hellas basin have intensified, and wind stresses for this key location are increased significantly over those of the baseline simulation.

References: *Shirley, J. H.* (2015), Solar system dynamics and global-scale dust storms on Mars, Icarus 252, 128-144, doi:10.1016/j.icarus.2014.09.038. *Shirley, J. H.*, (2016). Orbit-spin coupling and the circulation of the Mars atmosphere, http://arxiv.org/abs/1605.02707. *Mischna, M. A., and J. H. Shirley*, (2016). Numerical Modeling of Orbit-Spin Coupling Accelerations in a Mars General Circulation Model: Implications for Global Dust Storm Activity, http://arxiv.org/abs/1602.09137.

Acknowledgements: This work was performed at the Jet Propulsion Laboratory, California Institute of Technology, under a contract from NASA. Funding from NASA's Solar System Workings Program is gratefully acknowledged. Government sponsorship acknowledged.